Project no. 004089

AMMA

Instrument : IP

# D.2.1.A.l

# The 10 July 2006 case-study : Large-scale and single column modeling

*Single column modeling of selected AMMA SOP cases: diurnal cycle*

Due date of deliverable:
Actual submission date:
December 2009

Start date of project: 1st January of 2005 Duration: 60 months

Organisation name of lead contractor for this deliverable: **CNRM**

Prepared by F. Guichard, F. Couvreux, C. Rio (CNRM)

| Project co-funded by the European Commission within the Sixth Framework Programme (2002-2006) | | |
|---|---|---|
| **Dissemination Level** | | |
| **PU** | Public | |
| **PP** | Restricted to other programme participants (including the Commission Services) | X |
| **RE** | Restricted to a group specified by the consortium (including the Commission Services) | |
| **CO** | Confidential, only for members of the consortium (including the Commission Services) | |

# The 10 July 2006 case-study : large-scale and single column modeling

*Single column modeling of selected AMMA SOP cases: diurnal cycle*

F. Guichard, F. Couvreux and C. Rio

## 1) Context

An accurate modelling of the diurnal cycle of convection is still a challenge at large scale (Yang and Slingo 2001, Betts and Jakob 2002). This issue is particularly important over land where the diurnal cycle of convection is more pronounced (Nesbitt and Zipser 2004). A number of studies have underlined the major role of parametrizations in shaping the simulated diurnal cycles of convection. It has been often stated that daytime convection occurs too early in large-scale and parametrized models (Betts and Jakob 2002, Guichard et al. 2004, Bechtold et al. 2004, Rio et al. 2009), in response to the daytime increase of CAPE due to the daytime increase of boundary layer equivalent potential temperature (θe_bl).
In the deliverable D.2.1.A.k, a case-study of daytime initiation of convection was presented and analysed with AMMA SOP data of the 10 July 2006. This study demonstrates that daytime convection over flat semi-arid lands can initiate within an environment which contrasts radically with both the wet Tropics and mid-latitudes. In particular, no daytime increase of CAPE nor of θe_bl was observed. Rather, both decreased the 10 July prior to the initiation of convection.
Therefore, an main object of the present study is to investigate whether convection initiates or not in parametrized models for this case, and if yes when in the diurnal cycle.
First, results from two large-scale NWP models are presented, in order to better characterize the performance of such models. Then, two different single column models are used to simulate the case-study presented in D.2.1.A.k. Results are compared with LES of this same case.

## 2) Large-scale modelling

Maps of 24-h cumulative rainfall from the CRP-RFE2 satellite product are presented in Fig. 1 for the 8, 9 and 10 July 2006 for a 10° of longitude by 5° of latitude region enclosing the area where the convective system presented in D.2.1.A.k initiated and died (bottom plot, grey zone partly included in the blue rectangle surrounding Niamey). The 10 July, rainfall amounts were much reduced compared to the two previous day according to RFE2 and other satellite rainfall products (not shown) and occurred in the form of isolated spots of rain within an otherwise rain-free region.
Figure 2 shows the corresponding rainfall amounts predicted by ARPEGE-Tropiques (ARP-T) and AROME. None of them allows to capture the observed pattern, and both differ markedly from each other. This is emphasized by their distinct spatial resolution, but would still hold if AROME results were re-gridded on the coarser ARP-T grid. Rainfall is widespread in ARP-T, more spotty and intense in AROME. Overall, rain does not fall at the same places in the three maps (Fig. 2). In addition, spin-down issues are significant as illustrated in Fig. 3 for ARP-T: it rains much less the 10 July then, but not a the right places either.
It hardly rained in the ECMWF-IFS, which is characterised by a lack of rainfall in the Sahel, and this is still true of the ECMWF AMMA re-analysis even though the bias is somewhat reduced (Agusti-Panareda et al. 2009).
In summary, and not surprisingly, the small convective event under study was not forecast by NWPs, in so far as it can be well characterized by its rainfall as diagnosed from satellite data (three different satellite estimates were used, and the convective system is identified by all of them, not shown). On the other hand, there is no significant orographic feature over the area, and the variety of rainfall patterns among models suggest that orography-related mechanisms do not play a leading role in driving the patterns of simulated rainfall.

The vertical profiles of the ECMWF-IFS and AMMA re-analysis (analysis and forecast), and of AROME have been compared to soundings and flight data in order to assess whether and how their departure from observations could explain some of this result (see Figs. 4, 5 and 6 for ECMWF). The AMMA re-analysis displays higher southerly winds, it is also warmer except at 1800 UTC (e.g., Fig. 5, green and blue curves). These figures also shows how the forecast from the AMMA reanalysis (red solid curves) rapidly drifts from its analysis (blue line); it is drier in the boundary layer and moister above, this is associated with a weakening of the low level southerly, a strengthening of southerly wind above and a weaker AEJ (see for instance Fig. 5, 1200 UTC). At 1800 UTC, the low levels are warmer than all model-based estimates for reasons which are yet unclear (except in the lowest hundred metres where the sounding sampled the convective outflow). Thus, these results provide some elements of evaluation for models. They do not provide clue though on the actual convective sequences simulated by different models.

An attempt was carried out in in order to characterize better the local environments where it rained and those where it did not rain over the latitudinal band [12.5°,14°], from 12h to 21h in models. As an example, Fig. 4 summarizes for the ECMWF-IFS the vertical profiles of theta and qv in both areas and how they compare to the Niamey soundings (this is made possible owing to the fact that these profiles are provided at the (high) vertical resolution of the model). Differences in temperature are small. They are the more pronounced in the early morning (red versus yellow curves), but they have almost vanished by noon. In addition, even if advection appear as relatively small for this case study (see D.2.1.A.k) it cannot be neglected in the morning; this contributes to weaken the links between early morning *local* atmospheric structure and the subsequent daytime convection (these considerations also concern the strength and scale of the links between surface fluxes and convection). It seems that areas where it rained in the afternoon and evening where moister in the low levels at noon (compare green and grey curves), but without obvious differences in convective boundary layer heights. They are also warmer and slightly more humid above the boundary layer in the SAL below 4 km at 1800 UTC. Grid points where it did not rain display more mixing below 2km where they are, on average, warmer and drier at 1800 UTC. This would be consistent with the cooling induced by convective downdraughts and the moistening resulting from evaporation of rainfall within a thick and relatively dry mixed layer. These first results provide some indications regarding the drivers of rainfall in the model, and the approach should be developed further, in more details. However, daytime convection occurring in the model also results from a very different balance of processes, starting from surface processes. This is illustrated in Fig. 8 for surface sensible and latent heat fluxes. In particular, it suggests that the ECMWF model overestimates the surface latent heat flux as commonly found prior to the monsoon onset (Drusch and Viterbo 2007, Meynadier et al. 2010, Agusti-Panareda et al. 2010).

In summary, results presented above point to a lack of accuracy of NWP models in the simulation of daytime convection. In the present case of daytime convection in semi-arid conditions, this appears to be related to a complex balance of physical and advective processes. This is an additional motivation for the study presented in the next section, which makes use of a more simple and controlled modelling framework to assess the physical parametrizations of the model.

**3) Single column modelling**

In D.2.1.A.k, a case-study designed from observations and used to perform a three-dimensional large-eddy simulation was presented. Simulations from three single column models of this same case-study have been performed (see Table 1 for a summary of the main features of these SCMs). In short, surface sensible heat fluxes have been prescribed in the model, together with larger-scale horizontal advection and vertical velocity. The results are presented below.

A first question addressed by this study was whether deep convection was arising too earlier in this

semi-arid environment, as commonly found over cooler and more humid continental regions. Our first results suggest that it is still the case, at least for the models evaluated here (Fig. 9). In agreement with Rio et al. (2009), for this case too, the new physical package of LMDZ (LMDZ2) shift the onset of convection later in the early afternoon compared to the older one (LMDZ1). This involves the development of a deeper, more entraining convective boundary layer (signed by a stronger cooling at the top of the mixed layer). In both LMDZ2 and MesoNH, which make use of relatively close parametrizations of daytime boundary layer convection (referred to as dry and shallow convection in Table 1), the onset of deep convection occurs around 14h, i.e. later than in LMDZ1, but still some three hours earlier than in the LES. The differences of the daytime sequences are in fact fairly consistent with those discussed by Guichard et al. (2004).

In a second step, it is important to assess how these distinct timings of convection are, or not, associated with different boundary layer properties and convective indexes. At noon, prior to deep convection, there is a trend from cooler moister to drier warmer boundary layers if one successively considers LMDZ1, LMDZ2 and MesoNH (Fig. 10). However, LES lies in between LMDZ2 and MesoNH but convection occurs much later in this fine scale simulation, while it occurs at about the same time in LMDZ2 and MesoNH. By 1800 UTC, the low levels have been affected in distinct ways by the particular sequences of deep convection which took place in each simulation.

Series of higher frequency profiles more detailed information. The most striking difference between the LES and SCMs is found for relative humidity above the mixed layer. The SAL progressively and regularly moistens in the LES after noon, while it remains dry in the SCMs even before the onset of convection. In MesoNH, instead, it is the mixed layer which moistens more than the LES. Profiles of relative humidity from soundings display a distinct, more local view than LES domain-mean values. They indicate the presence of several strong spikes of RH, which are more suggestive of local remnants from cloud processes once they have evaporated, within an otherwise dry SAL; a SAL where mixing of water vapour is a slower process than in the convective boundary layer.

The analysis of boundary layer properties and convective indexes is delicate because it involves apparently small differences but which may result in large differences (at least this is what can be inferred from the analysis of sensitivities for one single model). In addition, observations are more sensitive to particular choices made to compute those quantities even if they are derived from profiles interpolated on a common vertical grid as done here, simply because models are more smoother than observations (e.g. Plfc estimate in top plot of Fig. 12).
The most significant difference between models and observations is that the simulated level of free convection (Plfc) decreases in the morning while this feature is much less obvious from the (too) few observations (red symbols in Fig. 12). One must also keep in mind that an apparently small difference of 30 mb represents about 300m, which is quite a large difference in terms of boundary layer height, Plfc or lifting condensation level (Plcl).

This is associated with higher boundary layer $\theta e$ (not shown) and CAPE, and lower CIN (Figs. 13 and 14) in the models. The difference is large. CIN remains above 0 in the LES until 13h, i.e. later than in SCMs. The high levels of CAPE could play a role in the early 'SCM-onset' of convection. However, in SCMs, deep convection starts just after the morning increase of CAPE, at time when it does not decrease much, as the CIN reaches 0. In contrast, in the LES, convection occurs later, in an late afternoon environment where the CAPE is much lower and where the mean CIN already started to increase. Thus, the close time series of boundary layer properties and convective indexes in LES and mesoNH are associated with a very different timing of deep convection (Figs. 12 to 14 versus Fig. 9). At this stage, It would be valuable to explore more in depth the functioning of the call to parametrizations and also to conduct sensitivity studies under lower CAPE conditions. The later could be done by testing the sensitivity to prescribed surface and larger scale advection.

## 4) Conclusion

The simulation of the case-study presented in D.2.1.A.k by NWP models and SCMs has been evaluated. This case can be seen as a generic case-study of daytime convection over a semi-arid land under weak synoptic-scale control. NWP models are found to be unable to properly capture such situations. However, the diversity of patterns displayed by those models precludes a comprehensive analysis of the sources of their differences.

The more controlled and simple framework designed from observations to simulate this case was used by three SCMs (1D version of large-scale models, here including turbulent and convective parametrizations), namely two versions of LMDZ 1D and MesoNH 1D.

These models appears to simulate deep convection too early in this case as previously found under wetter environments. However, prior to the onset of deep convection, the simulated boundary layer and convective indexes already display differences with observations, and these may play an important role in the diurnal cycle of deep convection. Therefore, additional sensitivity tests are needed. This could be carried out within this simple framework, by modifying the prescribed conditions, in particular the surface fluxes and advection.

Finally, daytime fluctuations of relative humidity displays significant difference above the mixed layer in LES and SCMs. The SAL is progressively moistened by shallow convection prior to deep convection, while it stays dry in SCMs, with moisture remaining confined to the mixed layer in these models. Whether this process plays, or not, a role in the subsequent onset of deep convection, our study points to the need for a more advanced representation of shallow convection in models, as this daytime sequence is quite typical of the region. Our result suggest that it may be an important mechanism for moistening the SAL, from which humidity can be transported at a larger scale. In parametrized SCMs, this mechanism is lacking.

REFERENCES


Agusti-Panareda, A., D. Vasiljevic, A. Beljaars, O. Bock, F. Guichard, M. Nuret, A. Garcia Mendez, E. Andersson, P. Bechtold, A. Fink, H. Hersbach, J.-P. Lafore, J.-B. Ngamini, D. J. Parker, J.-L. Redelsperger, A. Tompkins, 2009 : Radiosonde humidity bias correction over the West African region for the special AMMA reanalysis at ECMWF, Quart. J. Roy. Meteor. Soc., 135, 595 – 617.

Bechtold, P., E. Bazile, F. Guichard, P. Mascart, and E. Richard, 2001 : A mass flux convection scheme for regional and global models. Quart. J. Roy. Meteor. Soc., 127, 869-886.

Bechtold, P., Chaboureau, J.-P., Beljaars, A., Betts, A. K., Köhler, M., Miller, M. and Redelsperger, J.-L., 2004: The simulation of the diurnal cycle of convective precipitation over land in a global model. Quart. J. Roy. Meteor. Soc., 130, 3119-3137.

Cuxart, J., P. Bougeault and J.-L. Redelsperger, 2000:A turbulence scheme for mesoscale and large-eddy simulations. Quart. J. Roy. Meteor. Soc.,126: 1–30.

Drusch M. and P. Viterbo, 2007: Assimilation of screen-level variables in ECMWF's Integrated Forecast System: a study on the impact on the forecast quality and analyzed soil moisture, Mon. Wea. Rev., 135, 300-314.

Emanuel, K. A., 1991 A scheme for representing cumulus convection in large-scale models. J. Atmos. Sci. 48, 2313–2335.

Gounou, A., Couvreux, F., Guichard, F., Boone, A. & Kohler, M. 2009. Observation and modelling of continental diurnal cycles in West Africa. Third International AMMA Conference, July 20—24, Ouagadougou, Burkina Faso.

Grandpeix, J.-Y., and J.-P. Lafore, 2010:J. Atmos. Res., in press.

Guichard, F., J. C. Petch, J.-L. Redelsperger, P. Bechtold, J.-P. Chaboureau, S. Cheinet, W. Grabowski, H. Grenier, C. J. Jones, M. Koehler, J.-M. Piriou, R. Tailleux and M. Tomasini, 2004: Modelling the diurnal cycle of deep precipitating convection over land with CRMs and SCMs. Quart. J. Roy. Meteor. Soc., 130, 3139-3172.

Hourdin, F., et al., 2002: J. Atmos. Res.
Lafore, J.-P., and Coauthors, 1998 : The Meso-NH atmospheric simulation system. Part 1: Adiabatic formulation and control simulations. Ann. Geophys., 16, 90-109.
Mathon, V., and H. Laurent, 2001: Life cycle of Sahelian mesoscale convective cloud systems. QJRMS, 127, 377-406.
Pergaud, J. et al. 2009.
Rio C, F. Hourdin, J.-Y. Grandpeix and J.-P. Lafore, 2009: Shifting the diurnal cycle of parameterized deep convection over land. Geophys. Res. Lett., 26, L07809 [doi: 10.1029/2008GL036779]
Yamada (1983)

Table 1: summary of parametrizations used in the three single column models

| SCM | LMDZ1 | LMDZ2 | MesoNH |
|---|---|---|---|
| small scale turbulence | *Louis (1979)* | *Yamada (1983)* | *Cuxart et al. (2000)* |
| dry convection | / | *Hourdin et al. (2002)*<br>*Rio & Hourdin (2008)* | *Pergaud et al. (2009)* |
| shallow convection | *Emanuel (1991)* | | |
| deep convection | *Emanuel (1991)* | *Grandpeix & Lafore (2010)* | *Bechtold et al. (2001)* |

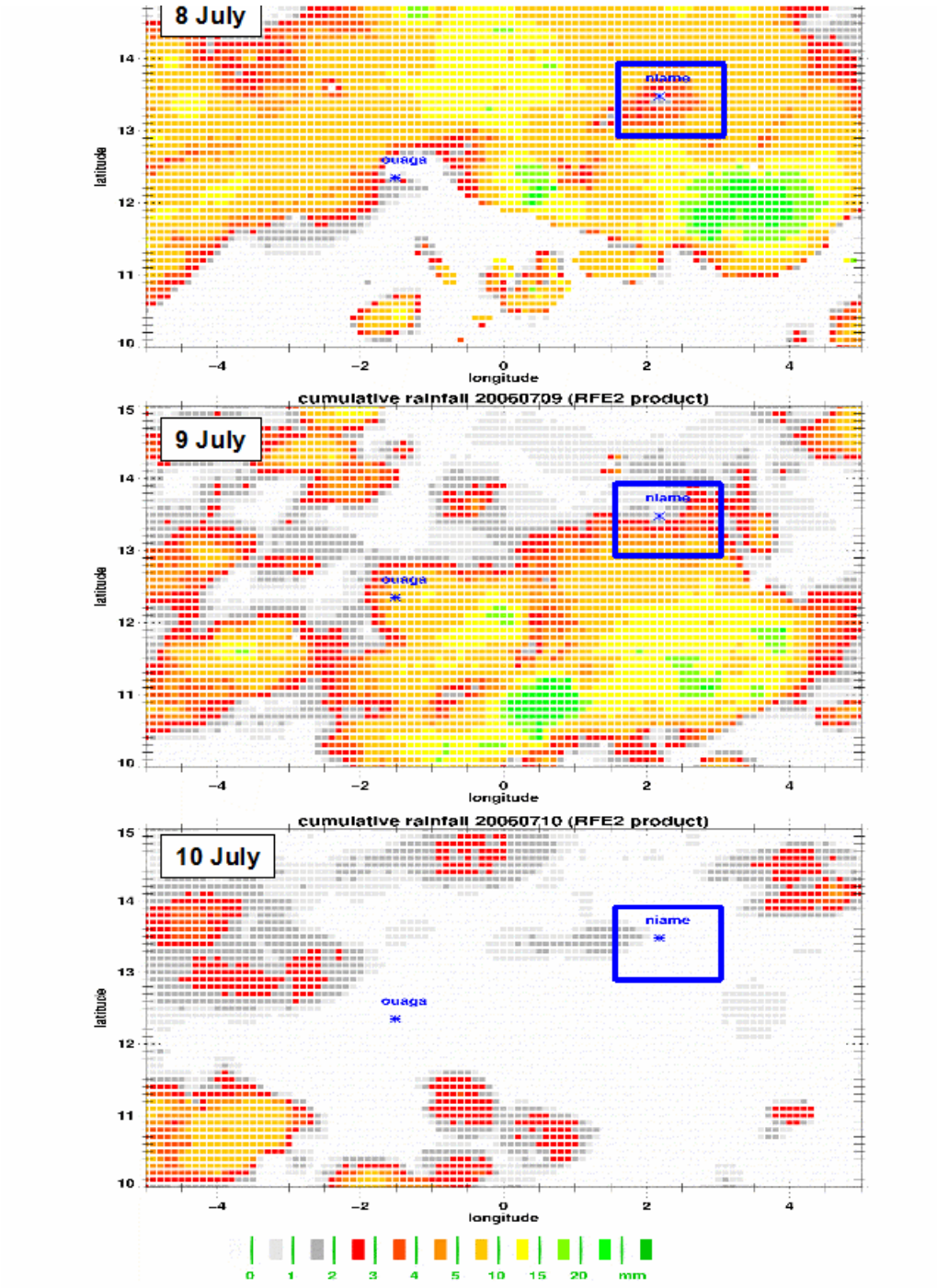


Figure 1 : rainfall maps from CPC-RFE2 (24-h cumulative rainfall) for 8, 9 and 10 July. (for day D, the 24-h time interval starts at 0600 UTC).

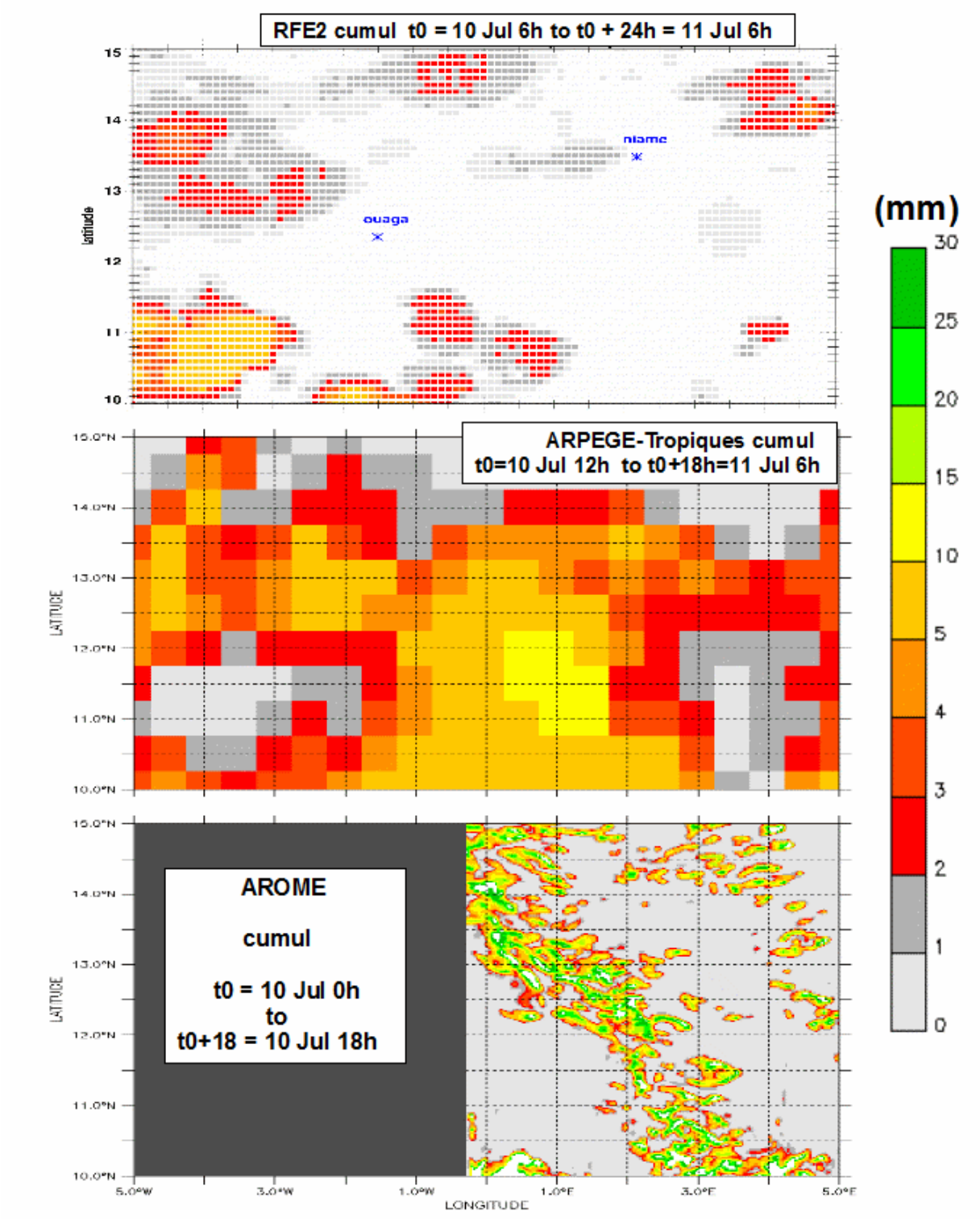


Figure 2 : Maps of cumulative rainfall, top: CPC-RFE2, 10 July 0600 UTC to 11 July 0600 UTC; middle: ARPEGE-Tropiques 10 July 1200 UTC to 11 July 0600 UTC and bottom: AROME, 10 July 0000 UTC to 10 July 1800 UTC. For ARPEGE-Tropiques and AROME, the initial (t0 on the plots) is also the time of start of the run.

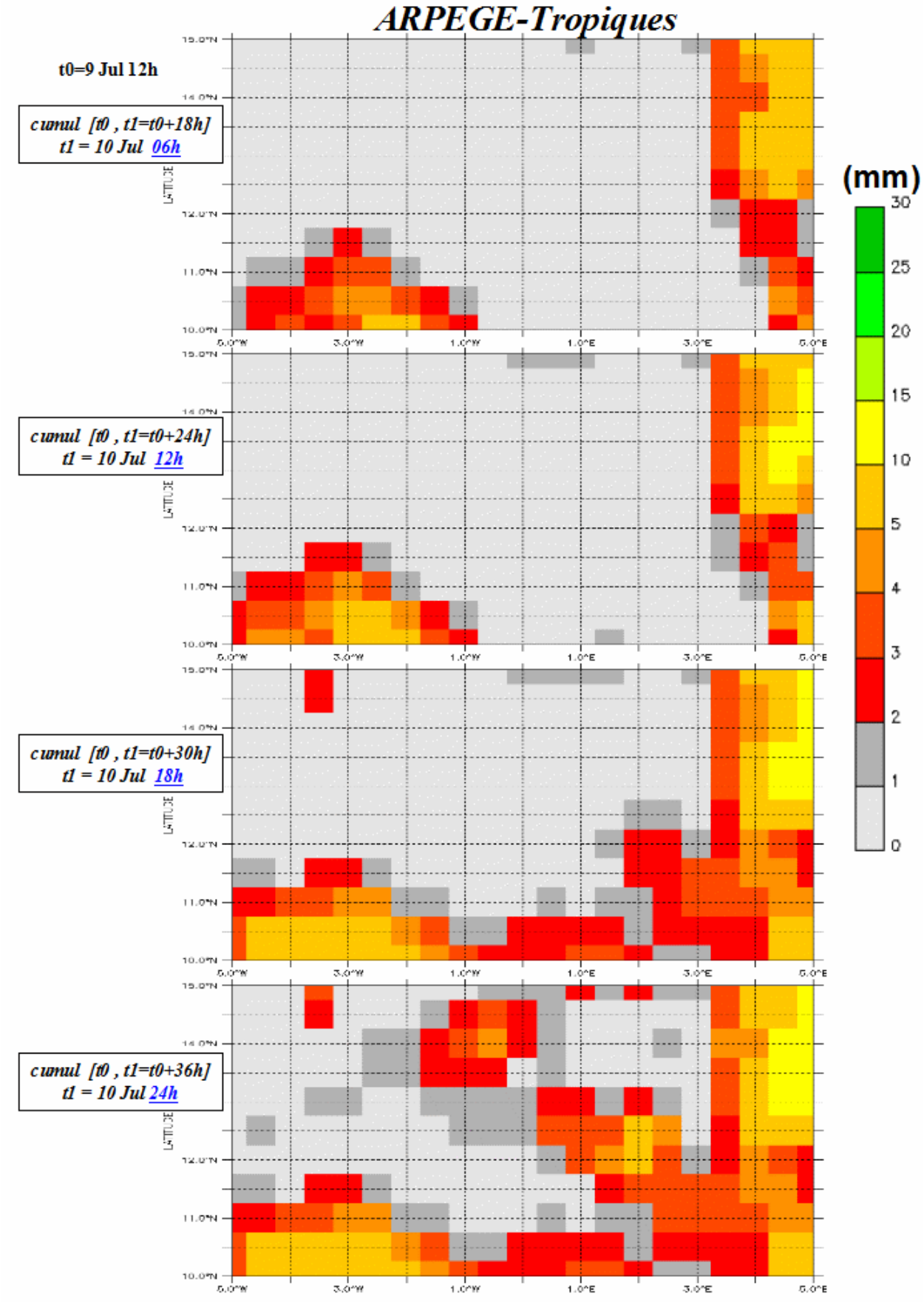


Figure 3 : successive (6-hourly sampled) cumulative rainfall amounts from the ARPEGE-Tropiques run started 9 July at 1200 UTC.

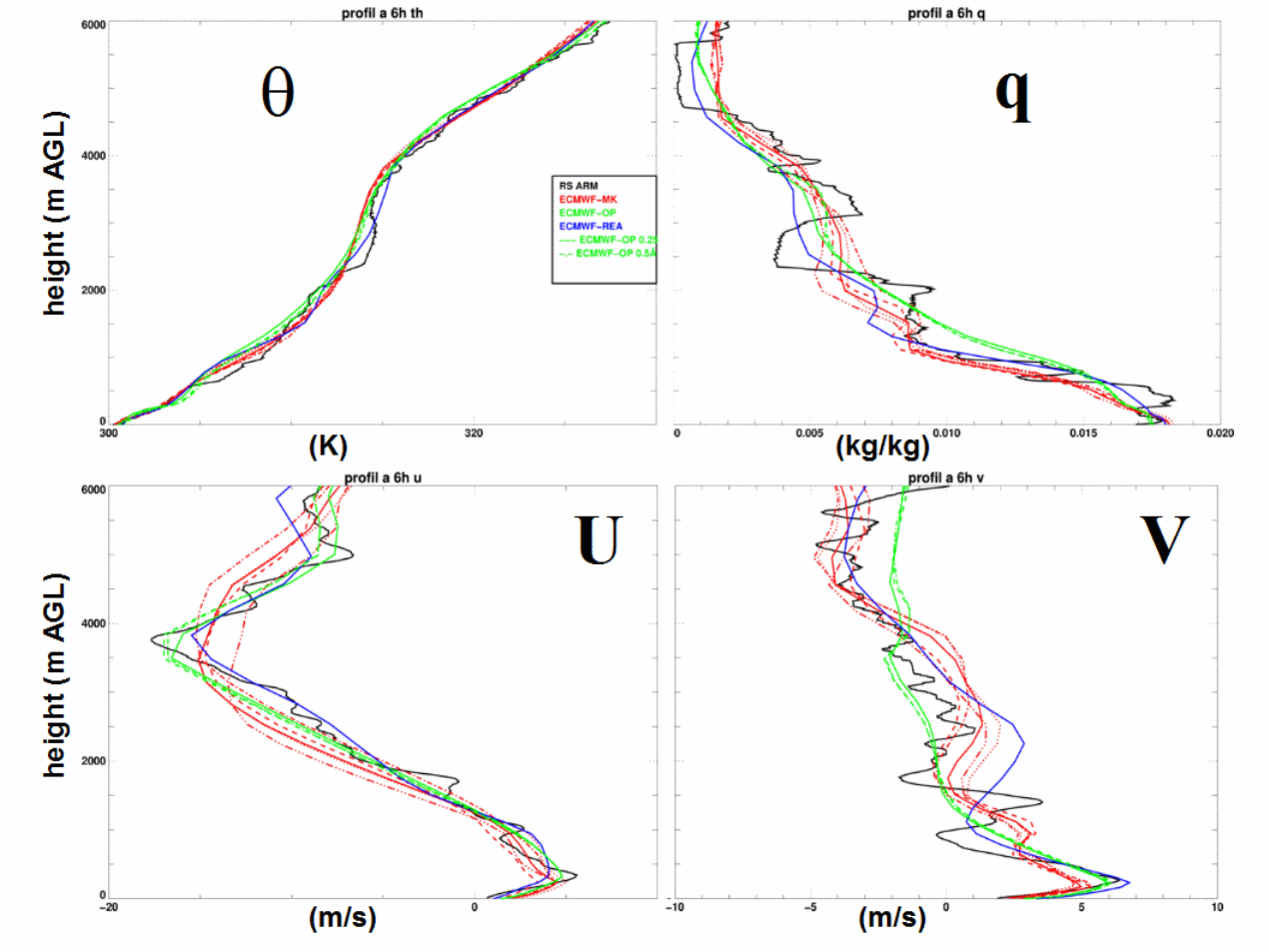


Figure 4 : vertical profiles of potential temperature (θ), specific humidity (q), zonal (U) and meridional (V) wind at Niamey (observations) or close by (aircraft data and models) at 0600 UTC; black: soundings, grey: aircraft data, green: ECMWF-IFS (analysis, the different line styles identify archives, extraction from MARS, CLIMSERV-AMMA, Meteo-France, which were all characterized by distinct horizontal resolutions), blue: AMMA-Reanalysis (analysis, CLIMSERV), and red: AMMA-Reanalysis (forecast, on the model grid, courtesy of M. Köhler, the closest point is in solid red line and the profiles from the four east (dotted line), west (dashed line), north (dashed-dotted line) and south (dashed-double-dotted line) surrounding points are also drawn).

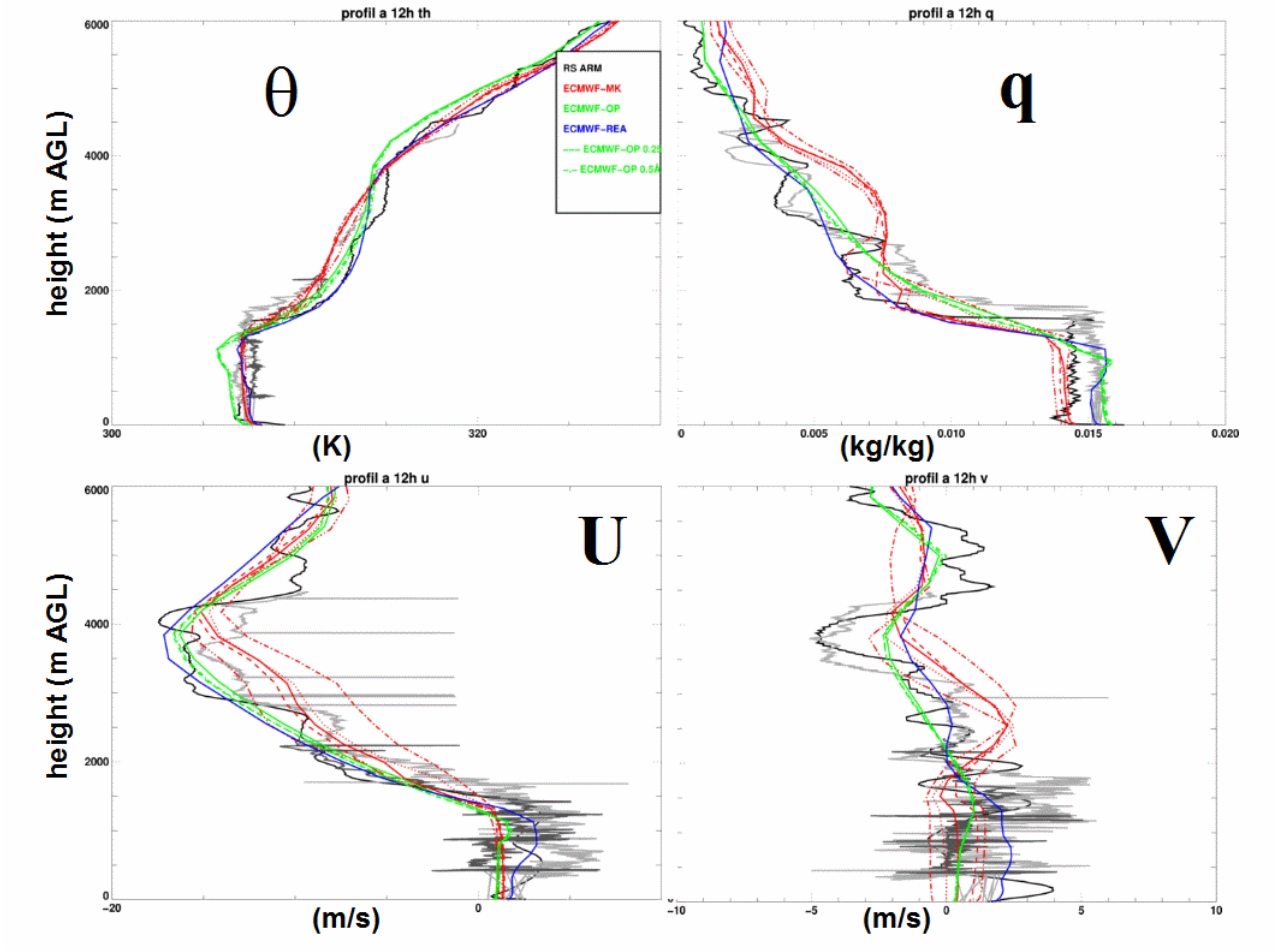


Figure 5 : same as previous figure except at or close to 1200 UTC.

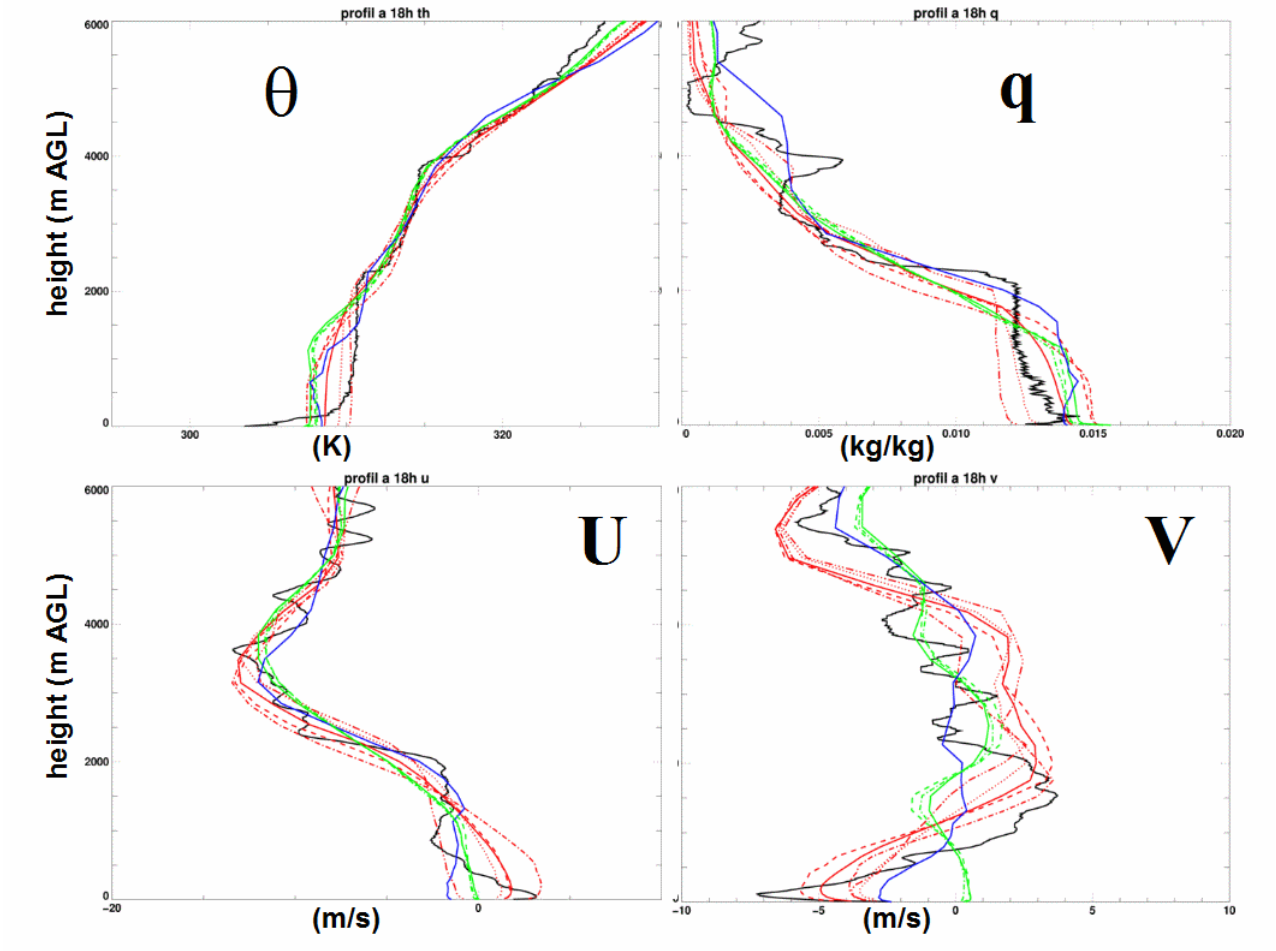


Figure 6 : same as previous figure except at or close to 1800 UTC.

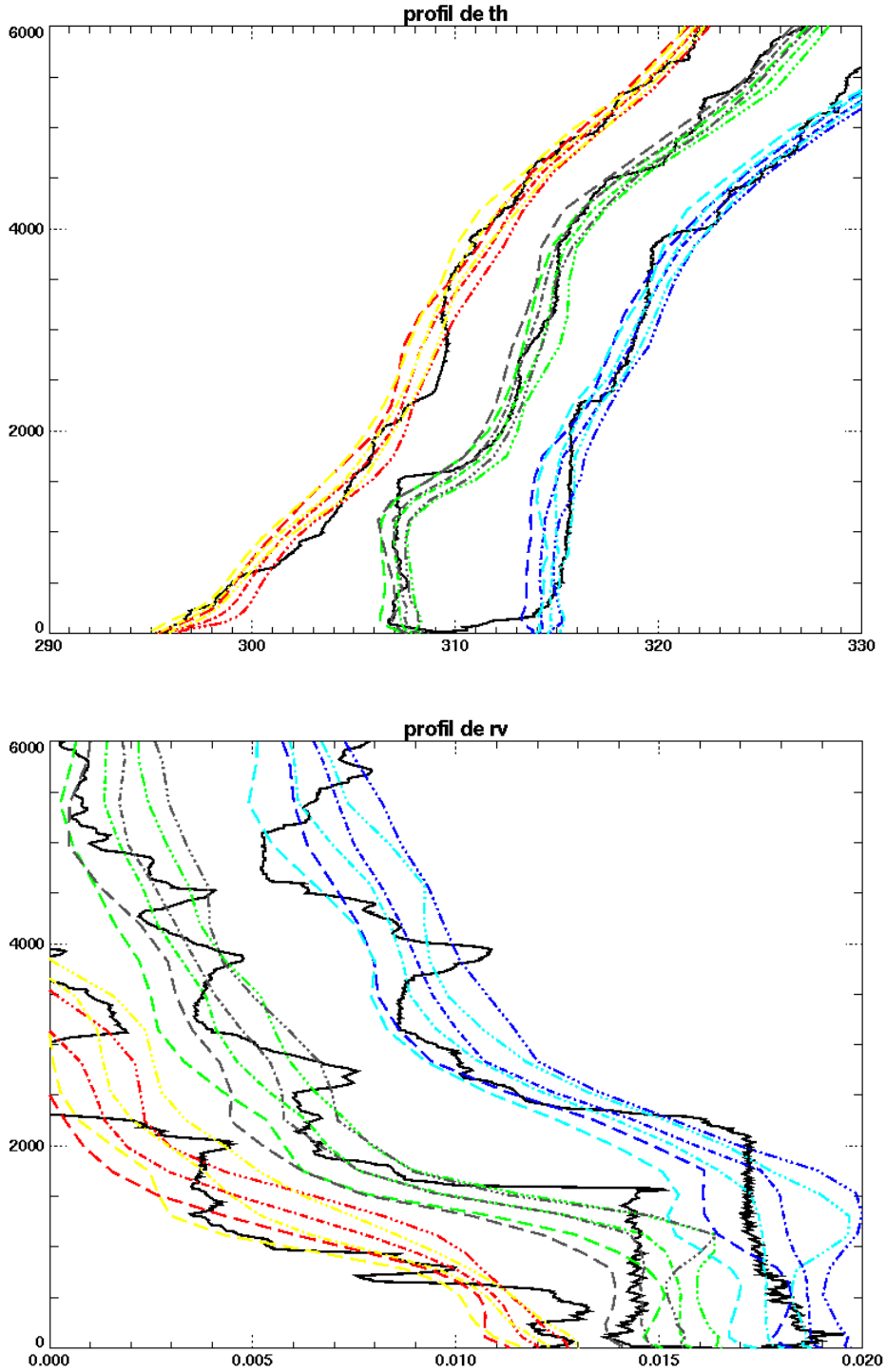


Figure 7 : profiles of potential temperature (top) and water vapour mixing ratio (bottom) : black: Niamey soundings, from 6h to 18h and colours: in the ECMWF for the same times. In the ECMWF, orange, green and blue lines (resp. yellow, grey and cyan) stand for the 6h, 12h and 18h profiles of the grid points where it rained from noon to 21h (resp. where it did not rain from noon to 21h). Grid points from the latitudinal band [12.5°,14°] are considered here. For each colour, the three lines correspond to the mean profile and to +/- standard deviations about the mean.

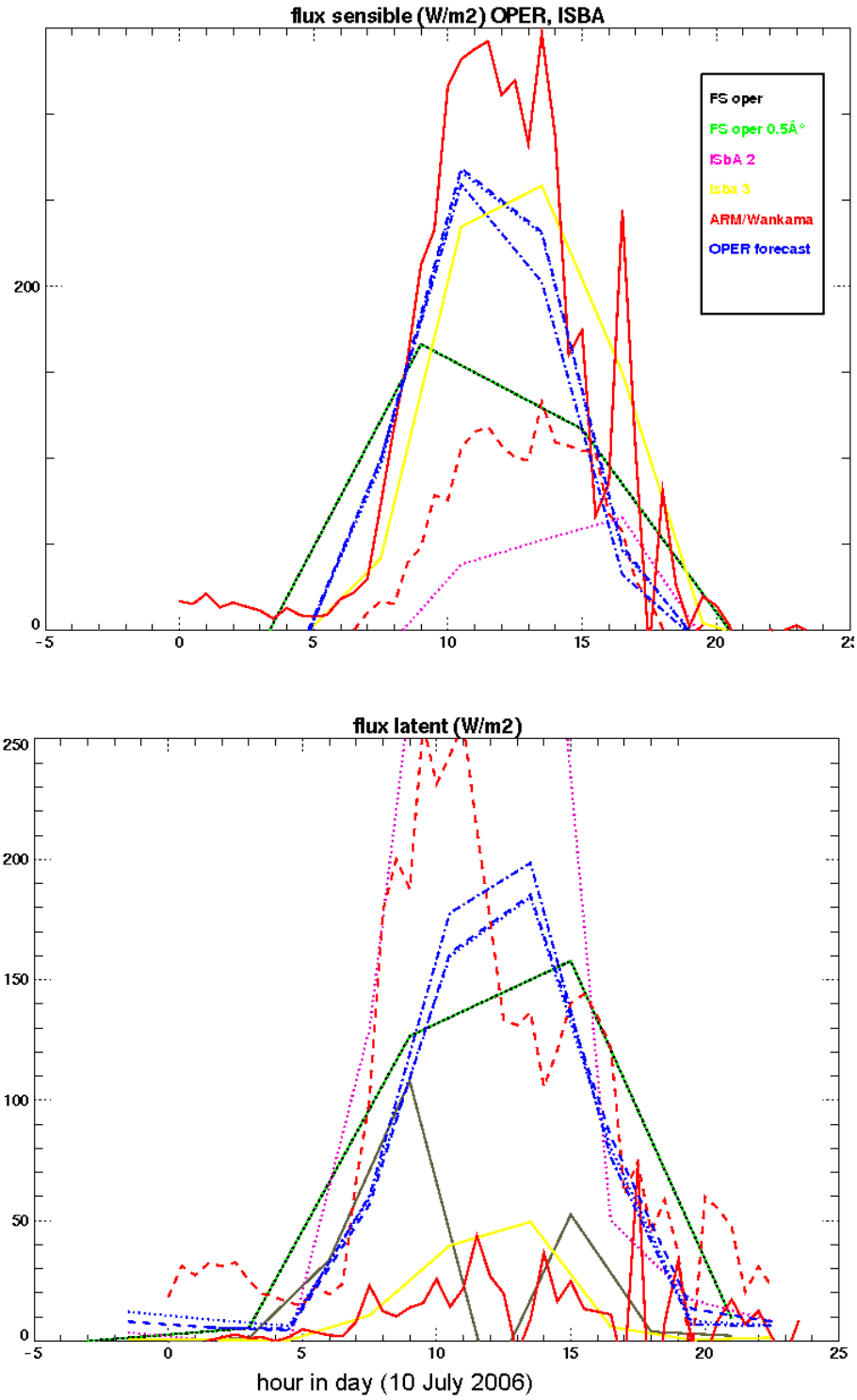


Figure 8: Surface sensible (top) and latent (bottom) heat fluxes at Niamey or its close vicinity; measured by the AMF in Niamey (red solid line) and by the flux station of Wankama (red dashed line) – 30-min sampling. Also shown are the fluxes predicted by ISBA in an off-line mode (3-h cumulative values), with prescribed rainfall, in pink EPSAT-SG and in yellow TRMM rainfall product); and the fluxes simulated by the ECMWF-IFS (green and black lines : within the spin-up time, 6-h cumulative fluxes; blue lines: after the spin-up time, estimated to be about 9 hours)

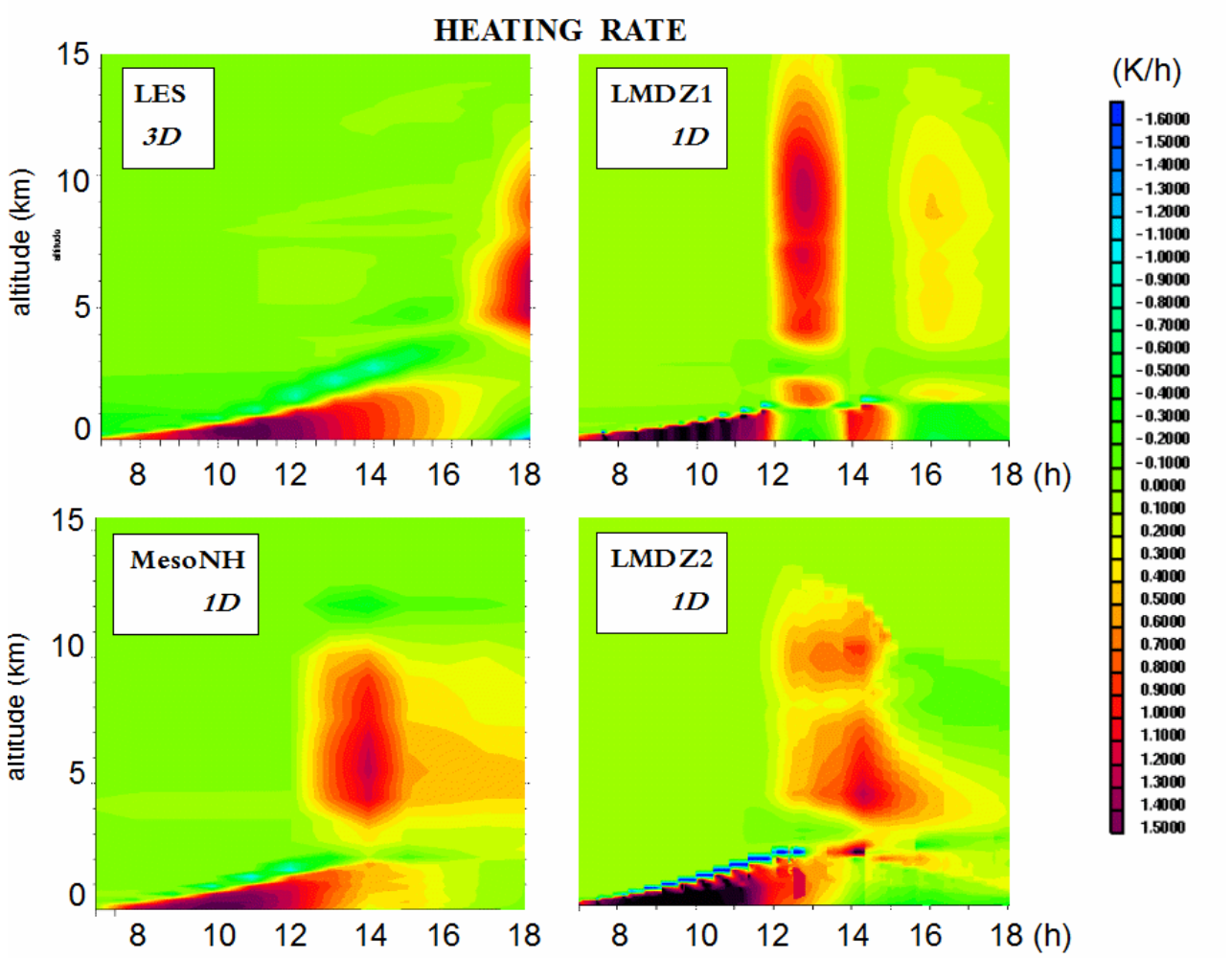


Figure 9: time-height diagrams of heating rates in the LES (top left) and the three SCM runs.

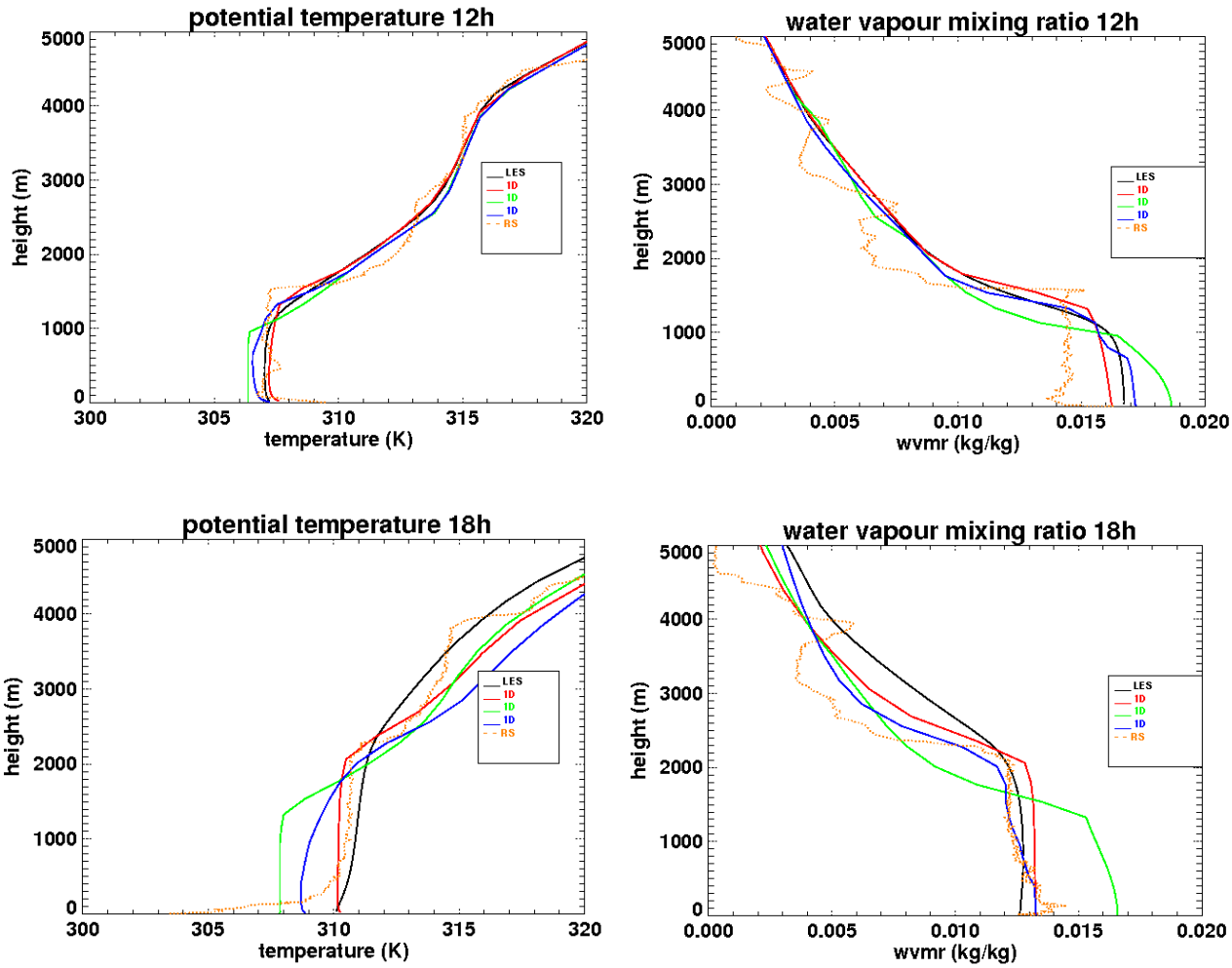


Figure 10 : vertical profiles of potential temperature (left) and water vapour mixing ratio (right) at 12h (top) and 18h (bottom); orange: Niamey soundings, black: LES, other colours: SCMs with green LMDZv1, blue: LMDZv2, red: MesoNH 1D.

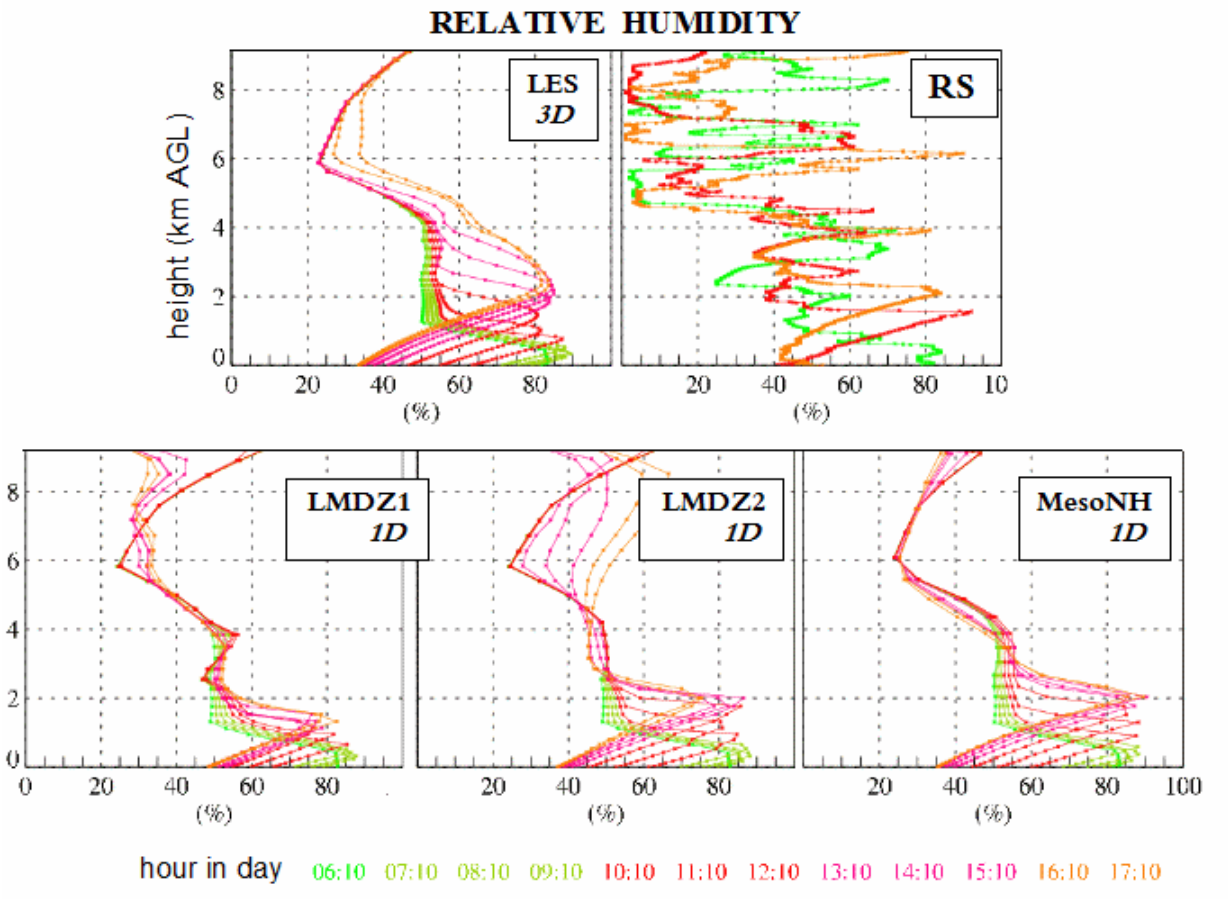


Figure 11: Vertical profiles of relative humidity during daytime the 10 July 2006; soundings (top right), LES (top left) and SCM runs (bottom). For the models, this is based on a 1-h sampling.

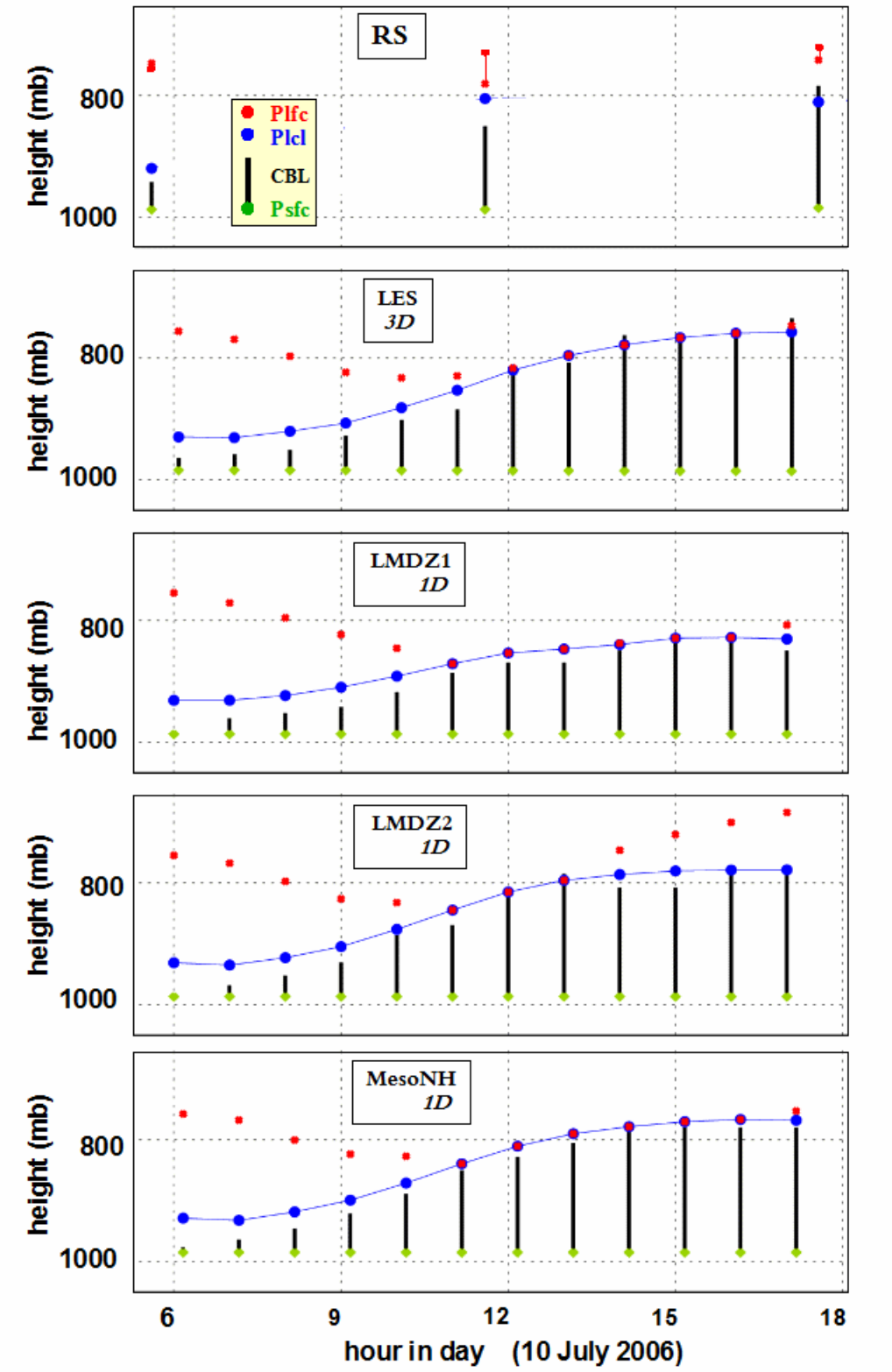


Figure 12: Time series of surface pressure (kaki symbol), convective boundary layer height (black line), lifting condensation level (Plcl blue disk) and level of free convection (Plfc, red symbol).

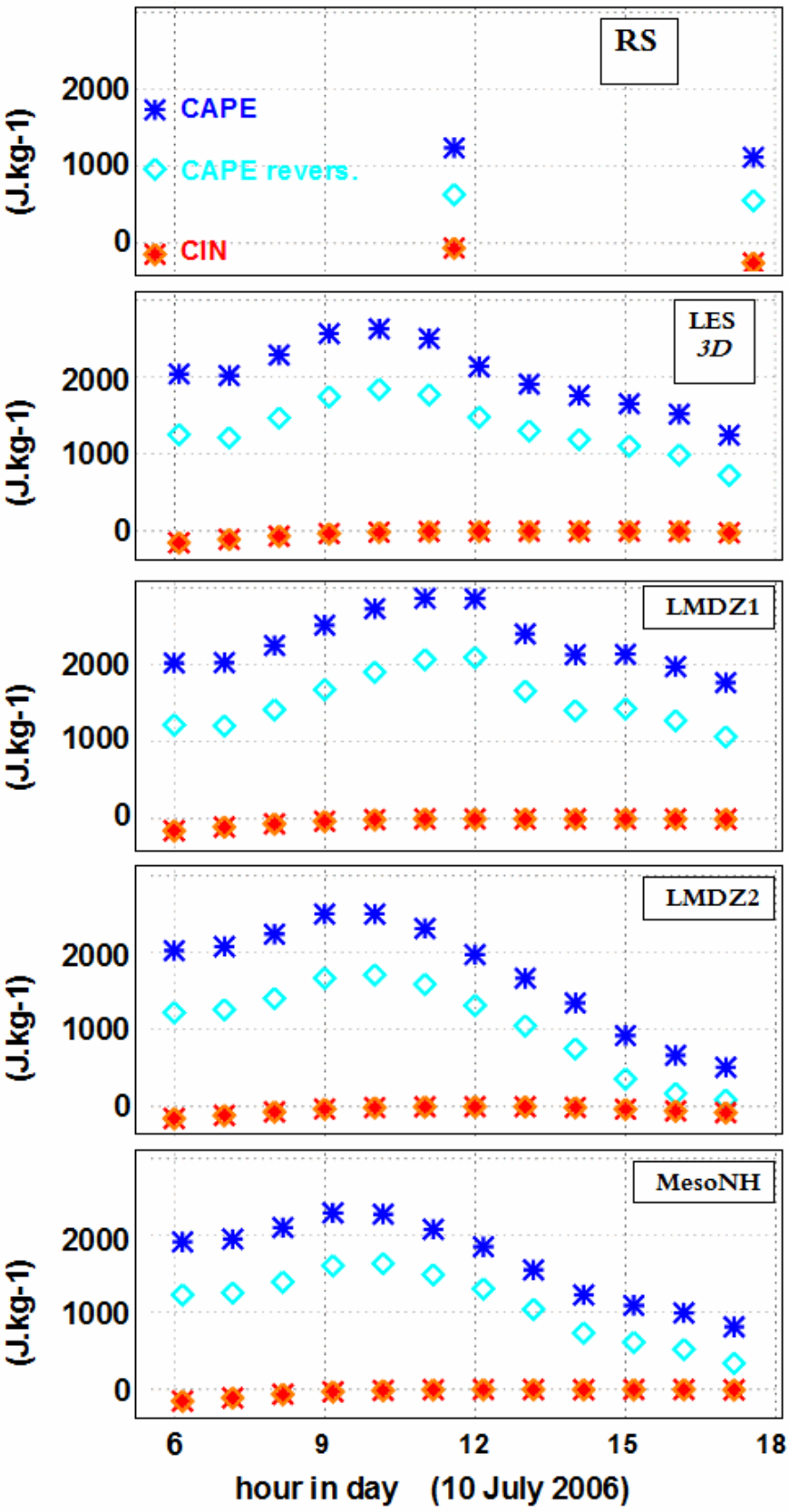


Figure 13: same as previous figure except for pseudo-adiabatic CAPE (blue stars), reversible CAPE (cyan diamonds) and CIN (orange symbols).

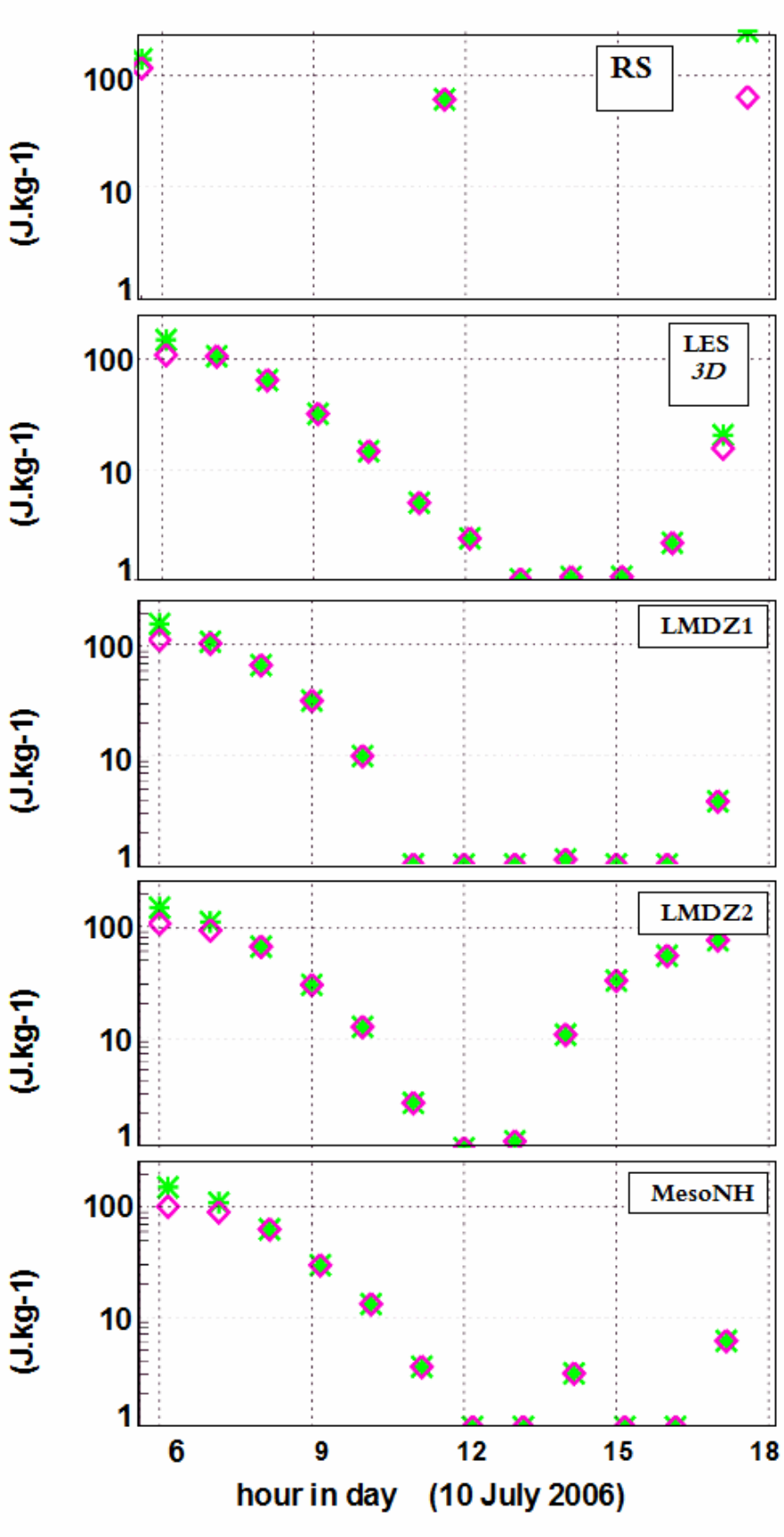


Figure 14 : Same as previous figure except for CIN, and using a logarithmic y-axis.